Article no. 14

THE CIVIL ENGINEERING JOURNAL 2-2018

MONITORING DYNAMIC GLOBAL DEFLECTION OF A BRIDGE BY MONOCULAR DIGITAL PHOTOGRAPHY

Guojian Zhang[1], Guangli Guo[1], Chengxin Yu[2], and Long Li[3,4]

1. *NASG Key Laboratory of Land Environment and Disaster Monitoring & School of Environmental Science and Spatial Informatics, China University of Mining and Technology, Daxue Road 1, 221116 Xuzhou, Jiangsu, P.R. China; g_j_zhang@cumt.edu.cn, guo_gli@126.com (Corresponding author)*
2. *Business School, Shandong Jianzhu University, Fengming Road 1000, 250101 Jinan, Shandong, P.R. China; ycx1108@126.com*
3. *School of Environmental Science and Spatial Informatics, China University of Mining and Technology, Daxue Road 1, 221116 Xuzhou, Jiangsu, P.R. China; long.li@cumt.edu.cn*
4. *Department of Geography, Earth System Science, Vrije Universiteit Brussel, Pleinlaan 2, 1050 Brussels, Belgium; long.li@vub.be*

ABSTRACT

This study uses MDP (monocular digital photography) to monitor the dynamic global deflection of a bridge with the PST-TBP (Photographing scale transformation-time baseline parallax) method in which the reference system set near the camera is perpendicular to the photographing direction and does not need parallel to the bridge plane. A SONY350 camera was used to shoot the bridge every two seconds when the excavator was moving on the bridge and produced ten image sequences. Results show that the PST-TBP method is effective in solving the problem of the photographing direction being perpendicular to the bridge plane in monitoring the bridge by MDP. The PST-TBP method can achieve sub-pixel matching accuracy (0.3 pixels). The maximal deflection of the bridge is 55.34 mm which is within the bridge's allowed value of 75mm. The MDPS (monocular digital photography system) depicts deflection trends of the bridge in real time, which can warn the possible danger of the bridge in time. It provides key information to assess the bridge health on site and to study the dynamic global deformation mechanism of a bridge caused by dynamic vehicle load. MDP is expected to be applied to monitor the dynamic global deflection of a bridge.

KEYWORDS

Monocular digital photography (MDP), Bridge health, Dynamic global deflection, Image sequences,Photographing scale transformation-time baseline parallax (PST-TBP) method

INTRODUCTION

Bridge deflection is an important basis to evaluate bridge health as it directly reveals the rigidity, stability, bearing capability and earthquake resistance of the bridge [1]. Bridge dynamic deflection can reflect the load impact coefficient and the internal force distribution of the structure [2]. It is therefore important to monitor the dynamic deflection of a bridge with a traffic light as it confronts heavier vehicle dynamic loads than others [3].

At present, there are many methods to monitor bridge deflection such as the precise levelling, the total station, the measurement robot, the laser speckle, the photographic imaging, the inclinometer method, GPS (Global Positioning System), the inertial measurement, the tension line method, the pipe deflection monitoring method and the photogrammetric techniques. The precise levelling can monitor the static bridge deflection with high precision, it is however out of monitoring the dynamic bridge deflection [4]. The total station can be used to monitor the deflection of a long-span bridge. It is however challenging to monitor the bridge dynamic deflection [5]. Although the measurement robot can monitor the instantaneous coordinates of a single point, it only can monitor the short periodic deflection of the bridge as it continuously monitors the same point two times with a periodic [6]. The laser speckle and the photographic imaging can monitor the dynamic deflection of a point on the bridge without monitoring the dynamic global deflection of a bridge [7, 8]. The inclinometer can monitor the bridge dynamic deflection with high precision, but it requires the installation shaft parallel to the bridge axis which is difficult to carry out in the field [9]. GPS can be used to monitor a long-span bridge as it has a low accuracy in monitoring the dynamic deflection of a bridge [10]. The inertial measurement has a high-resolution ability, but it is ineffective in low frequency [11]. The tension line method cannot monitor the global dynamic deflection of a bridge as one tension line only can monitor the deflection of one point [12]. The pipe method can monitor the static global deflection of the bridge, but it is not flexible in monitoring the dynamic deflection of a bridge yet [13]. Photogrammetric techniques [14, 15] can monitor the global deflection of a bridge, and it has advantage in non-contact measuring. But it cannot monitor the dynamic global deflection of a bridge as it uses two cameras or takes images from at least two different positions by one camera [16].

As such, a specific method is required to monitor the dynamic global deflection of a bridge and warn the possible danger of the bridge in time. MDP offers the potential to solve this problem [17, 18]. MDP, combining close range photogrammetric technique [19-21] with information technology [22, 23], can monitor dynamic global deflection of a bridge and obtain image sequences of a bridge as it continuously monitors a bridge by a single digital camera. Although it has not been as popular in bridge structures as the photogrammetric techniques, many pioneering applications in this field have proved its increasing capability [24, 25].

It is clear that in most of the previous studies MDP had been used in monitoring bridge deflection. However, they did not consider problems such as digital camera parallaxes caused by the environment and the photographing direction being un-perpendicular to the bridge plan.

The aim of this study is to propose the PST-TBP (photographing scale transformation-time baseline parallax) method in MDP to monitor the dynamic global deflection of a bridge to grasp the deflection characteristics of the bridge caused by vehicle dynamic load and MDPS (monocular digital photography system) is used to depict the deflection trend curves of the bridge in real time to assess bridge health on site and warn the possible danger.

MONOCULAR DIGITAL PHOTOGRAPHY SYSTEM

Accuracy assessment of a digital camera

This study uses DLT (direct linear transformation) method to assess the digital camera accuracy [26]. Firstly, eight or more reference points with weights are properly distributed in the laboratory. Then, we used the indirect adjustment method to calculate the data with consideration of L coefficients. The DLT method model is expressed as (1)：

$$\left.\begin{aligned} x-\frac{L_1X+L_2Y+L_3Z+L_4}{L_9X+L_{10}Y+L_{11}Z+1}=0 \\ z-\frac{L_5X+L_6Y+L_7Z+L_8}{L_9X+L_{10}Y+L_{11}Z+1}=0 \end{aligned}\right\} \tag{1}$$

where *x* and *z* are image plane coordinates of deformation points without errors, *X, Y* and *Z* are the space coordinates of the correspondence deformation points, and *Li (i =1,2,3,…,11)* are the functions of the exterior and interior parameters of a digital camera.

The error (2) can be obtained by linearizing Equation (1):

$$v=\begin{pmatrix} P_1V_1 \\ P_2V_2 \end{pmatrix}=\begin{pmatrix} M & N_0 \\ 0 & I \end{pmatrix}\begin{pmatrix} \Delta L \\ \Delta X \end{pmatrix}-\begin{pmatrix} W_1 \\ 0 \end{pmatrix} \tag{2}$$

where *P1* and *P2* are the weight matrices of image point observations and the reference point observations, respectively, ΔX is the correction matrix of the reference points, N_0 is the coefficient matrix of ΔX, *M* is the coefficient matrix of ΔL, and W_1 is the constant matrix of image point observations.

In Table 1, the calculation distances of U0-U2, U1-U3, and U2-U4 were obtained by the DLT method. Measurement distances of U0-U2, U1-U3, and U2-U4 were seen as precise values. The measurement errors were obtained by differencing the calculation distance with the corresponding measurement distance. The maximal measurement error of the digital camera is within 1mm which meets the accuracy requirements of deformation monitoring [27].

Tab. 1 - Measurement error/mm

Line	U0-U2	U1-U3	U2-U4
Calculation distance	588	596	599
Measurement distance	589	595	599
difference	1	1	0

A principle of photographic scale transformation

The photographic scale of somewhere always changes along the photographing distance (from the position to the photography centre) [28, 29]. Figure 1 shows a schematic diagram of a CCD (Charge Coupled Device) camera capturing images at different photographing distances *H3* and *H4*. *H1* is the focal length of a CCD camera, *H2* is the distance between the optical origin (o) and the front end of CCD camera, *D1* on reference plane and *D2* on object plane are the real-world length formed by the view field of the CCD camera at photographing distances *H3* and *H4* respectively, and *N* is the maximal pixel number in a horizontal scan line of an image plane, which is fixed and known as a priori irrelevant of the photographing distances.

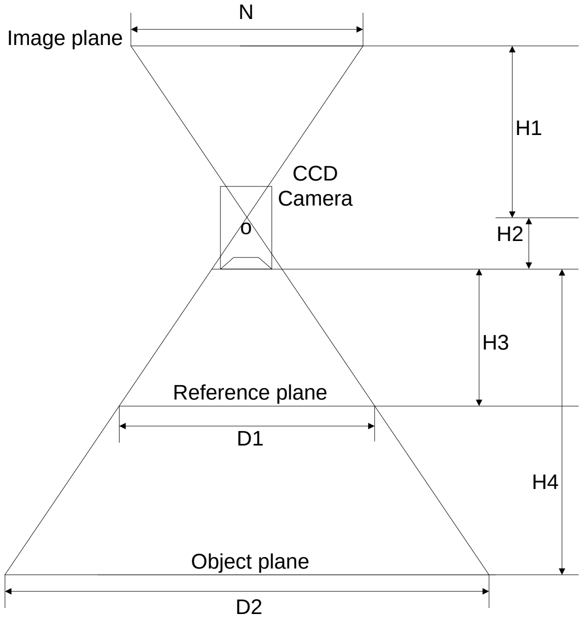

Fig. 1 - Schematic diagram of photographing scale transformation

Based on Figure 1, the relationship between pixel counts and distances can be described by:

$$\left.\begin{array}{l}\frac{H1}{H2+H3}=\frac{N}{D1}\\ \frac{H1}{H2+H4}=\frac{N}{D2}\end{array}\right\} \tag{3}$$

In general, *H3* and *H4* are meter-sized, while *H2* is centimetre-sized. Assume that *H2* can be ignored when the camera is far from the bridge, Equation (3) can be expressed as:

$$\left.\begin{array}{l}\frac{H1}{H3}=\frac{N}{D1}\\ \frac{H1}{H4}=\frac{N}{D2}\end{array}\right\} \tag{4}$$

From Equation (4), we have:

$$D2=\frac{H4}{H3}\cdot D1 \tag{5}$$

Assume that *M1* and *M2* are the photographing scale of the reference plane and the object plane, respectively. According to Equation (5), we have:

$$M2=\frac{H4}{H3}\cdot M1 \tag{6}$$

Namely,

$$M2=\Delta PSTC\cdot M1 \tag{7}$$

where $\Delta PSTC$ is the photographing scale transformation coefficient, and $\Delta PSTC=\frac{H4}{H3}$

Photographing scale transformation-time baseline parallax method

Assume that there are no errors in the measurement, the horizontal and vertical displacements of deformation point on object plane based on the time baseline method are given by:

$$\left.\begin{aligned}\Delta X^{PST} = M \cdot \Delta PSTC \cdot \Delta P_x = M^{PST} \Delta P_x \\ \Delta Z^{PST} = M \cdot \Delta PSTC \cdot \Delta P_z = M^{PST} \Delta P_z\end{aligned}\right\} \tag{8}$$

where ΔX^{PST} and ΔZ^{PST} are the horizontal and vertical deformation of a deformation point on the object plane, ΔP_x and ΔP_z are the horizontal and vertical displacements of the corresponding deformation point on the image plane, M is the photographic scale on the reference plane, and M^{PST} is the photographing scale on the object plane. Note that ΔP_x and ΔP_z are with parallax errors.

However, a time baseline parallax method requires the photographing direction perpendicular to the bridge plane and the camera constantly when a single-digital camera is used to monitor the bridge. It is difficult to carry out [30]. This study proposes the PST-TBP (photographing scale transformation-time baseline parallax) method to solve these problems.

The PST-TBP method consists of three steps. Firstly, the TBP method is used to get the displacements on the reference plane of deformation points. These displacements are with the parallax errors caused by the change of intrinsic and extrinsic parameters of a digital camera. Secondly, reference points are used to match a zero image with the successive images to eliminate the parallax errors. And the corrected displacements on the reference plane are obtained. Lastly, the real displacements on the object plane of deformation points are equal to the corrected displacements on the reference plane multiplied by the photographing scale transformation coefficient. The details are as follows:

The first step, when a point on an object plane moves from A to B (Figure 2), its horizontal and vertical displacements on reference plane are given by:

$$\left.\begin{aligned}\Delta X = M \cdot \Delta P_x \\ \Delta Z = M \cdot \Delta P_z\end{aligned}\right\} \tag{9}$$

where ΔX and ΔZ are the horizontal and vertical displacements on reference plane of a deformation point, ΔP_x and ΔP_z are the horizontal and vertical displacements on image plane of deformation point, and M is the photographing scale on the reference plane. Note that ΔP_x and ΔP_z are with parallax errors.

In the second step, some points are laid at a stable position around the camera to form a reference plane which is perpendicular to the photographing direction, and the parallax is therefore eliminated through differencing a zero image with the successive images based on reference plane, respectively.

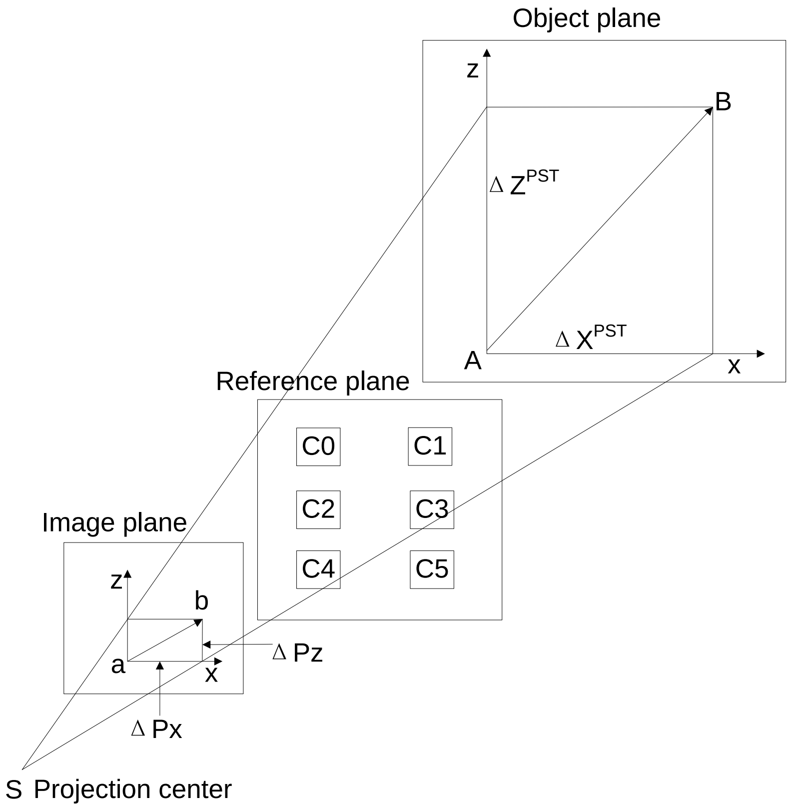

Fig. 2 - Photographic scale transformation-time baseline parallax method

The reference plane (Figure 2) consists of six reference points labeled as C0-C5 (at least three reference points), and the reference plane equation can be expressed as :

$$\left.\begin{aligned} P_x &= a_x x + b_x z + c \\ P_z &= a_z x + b_z z + d \end{aligned}\right\} \tag{10}$$

where *(x, z)* and $(P_x,\ P_z)$ are the image plane coordinates and the image plane parallaxes of a reference point, respectively. (a_x, b_x) and (a_z, b_z) are the parallax coefficients in *x* and *z*-direction respectively. *(c, d)* are the constant parallax coefficients in *x* and *z*-direction, respectively.

After correcting the displacements on the image plane of a deformation point based on the parallaxes of the reference plane, the corrected displacements on the image plane of a deformation point is obtained:

$$\left.\begin{aligned} \Delta P'_x &= \Delta P_x - P_x \\ \Delta P'_z &= \Delta P_z - P_z \end{aligned}\right\} \tag{11}$$

where $(\Delta P'_x, \Delta P'_z)$ and $(\Delta P_x, \Delta P_z)$ are the corrected displacements and the measured displacements on the image plane of a deformation point, respectively.

Thus, we obtained the corrected deformation values on the reference plane of a deformation point:

$$\left.\begin{aligned} \Delta X' &= M\Delta P'_x \\ \Delta Z' &= M\Delta P'_z \end{aligned}\right\} \tag{12}$$

where $(\Delta X', \Delta Z')$ are the corrected deformation values on the reference plane of a deformation point.

DOI 10.14311/CEJ.2018.02.0014

The last step is obtaining the corrected displacements on the object plane of a deformation point:

$$\left.\begin{aligned}(\Delta X^{PST})' = \Delta PSTC \cdot \Delta X' \\ (\Delta Z^{PST})' = \Delta PSTC \cdot \Delta Z'\end{aligned}\right\} \quad 13)$$

where $(\Delta X^{PST})'$and $(\Delta Z^{PST})'$ are the corrected displacements on the object plane of a deformation point.

In order to perform the PST-TBP method, a data processing toolkit has been developed in the environment of Microsoft Visual C++ 6.0. It allows synchronization of measuring pixel coordinates of deformation points and data processing. The monocular digital photography system consists of functions of solving data, storing data and displaying deformation curves, etc. The procedure of the toolkit is detailed in Figure 3.

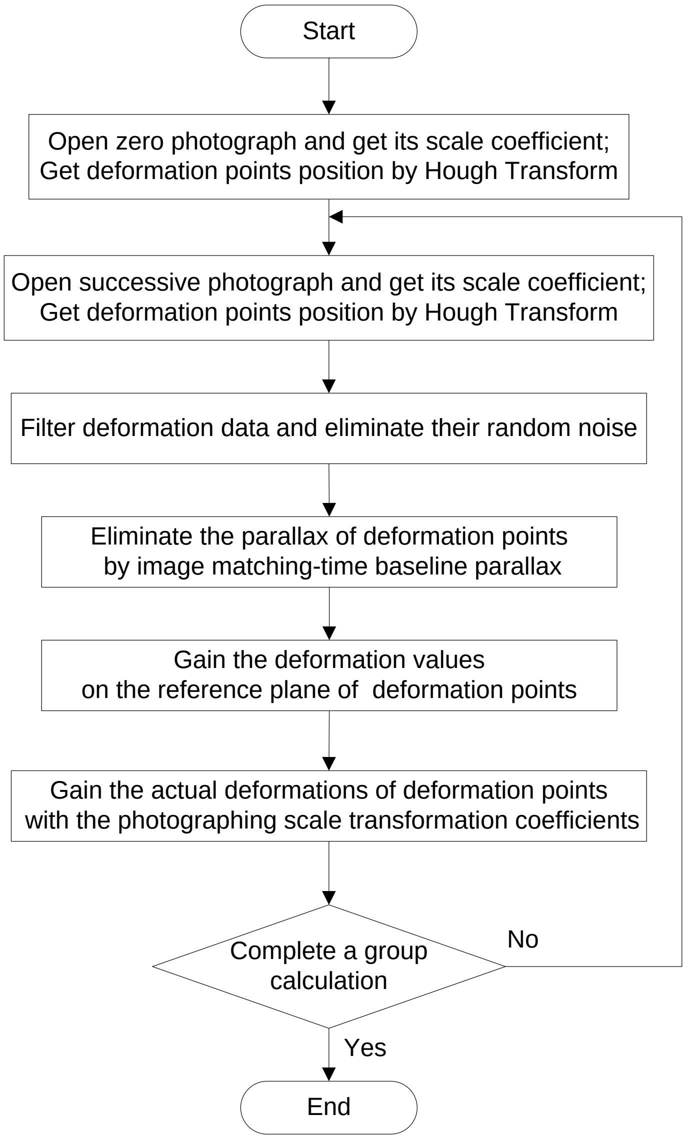

Fig. 3 – Flow chart of data processing

BRIDGE TEST

Figure 4 shows an early stage of the Fenghuangshan road bridge which is a self-balanced reinforced concrete, central bearing frame arch. This bridge has a 60-meter span, and a 31.5meter march made of steel tube concrete. Its deck is equipped with motor vehicles, facilities, slow lane, sidewalks and guardrails.

Before the test, we set the total station and three digital cameras on the specified position of the south side of the Xiaoqing river. To facilitate the stress analysis of this bridge and the field condition, six deformation point targets labelled as U0-U5 were set on the bridge's superstructure, and seven deformation point targets labelled as U6-U12 were evenly set on the bridge's major deck. Reference points labelled as C0-C1, forming the reference system, were set near the digital camera whose view is in Figure 4. The reference system, used to match a zero image with the successive image, is perpendicular to the photographing direction.

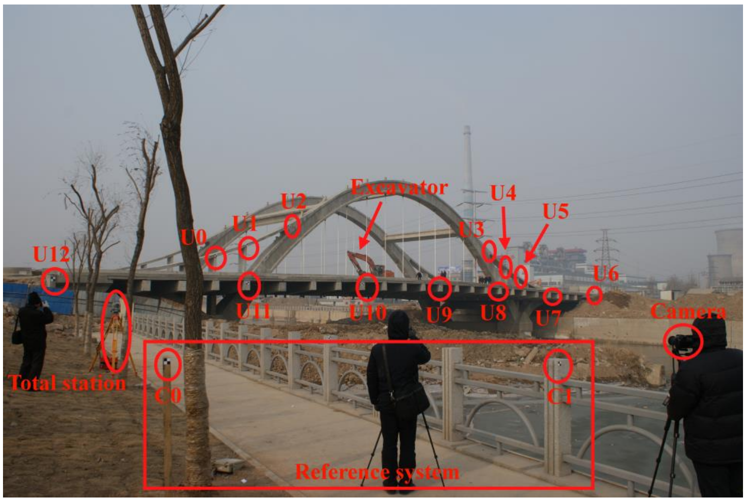

Fig. 4 - Field test on the Fenghuangshan road bridge (taken on July 16, 2009)

In the bridge test, the SONY350 cameras were held constantly as much as possible. The cameras used in this test can capture the instantaneous deflection of a bridge in 1‰ second and shoot this bridge seven times in one second. The test process was described as follows:

(1) In the test, one excavator moved on the deck at a speed of 20km/h from the north to the south. The cameras were used to shoot the bridge to produce the zero images before the excavator on the bridge.

(2) The cameras were used to shoot the bridge every two seconds when the excavator was moving on the bridge. Finally, ten successive images were produced.

(3) The total station was used to obtain the spatial coordinates of reference points and deformation points after the test.

Table 2 shows the two-dimension coordinates of selected monitoring points and camera as the elevation can be ignored in the study.

Tab. 2 - Spatial coordinates of selected monitoring points and camera

Name	Camera	C0	C1	C2	U6	U9	U12
X/m	8809.216	8806.411	8800.765	8806.206	8737.778	8748.484	8760.244
Y/m	14818.612	14820.39	14824.41	14824.41	14912.62	14867.6	14820.76

DATA PROCESSING AND ANALYSIS

Photographing scales of deformation points

Based on the photographing scale transformation, the photographing scales of U6, U9, and U12 can be expressed as:

$$\left.\begin{aligned} M_{U6}^{PST} &= M_0 \cdot \Delta PSTC_{U6} \\ M_{U9}^{PST} &= M_0 \cdot \Delta PSTC_{U9} \\ M_{U12}^{PST} &= M_0 \cdot \Delta PSTC_{U12} \end{aligned}\right\} \tag{14}$$

where M_{U6}^{PST}, M_{U9}^{PST} and M_{U12}^{PST} are the photographing scales of U6, U9 and U12 after the photographing scale transformation，respectively; M_0 is the photographing scale on the reference plane; $\Delta PSTC_{U6}$, $\Delta PSTC_{U9}$ and $\Delta PSTC_{U12}$ are the photographing scale transformation coefficients of U6, U9, and U12, relative to the reference plane.

$\Delta PSTC_{U6}$, $\Delta PSTC_{U9}$ and $\Delta PSTC_{U12}$ can be expressed as:

$$\left.\begin{aligned} \Delta PSTC_{U6} &= \frac{OD}{OA} \\ \Delta PSTC_{U9} &= \frac{OC}{OA} \\ \Delta PSTC_{U12} &= \frac{OB}{OA} \end{aligned}\right\} \tag{15}$$

where OA, OB, OC, and OD are the photographing distances of the reference plane, U12, U9, and U6, relative to the camera. They are detailed in Figure 5.

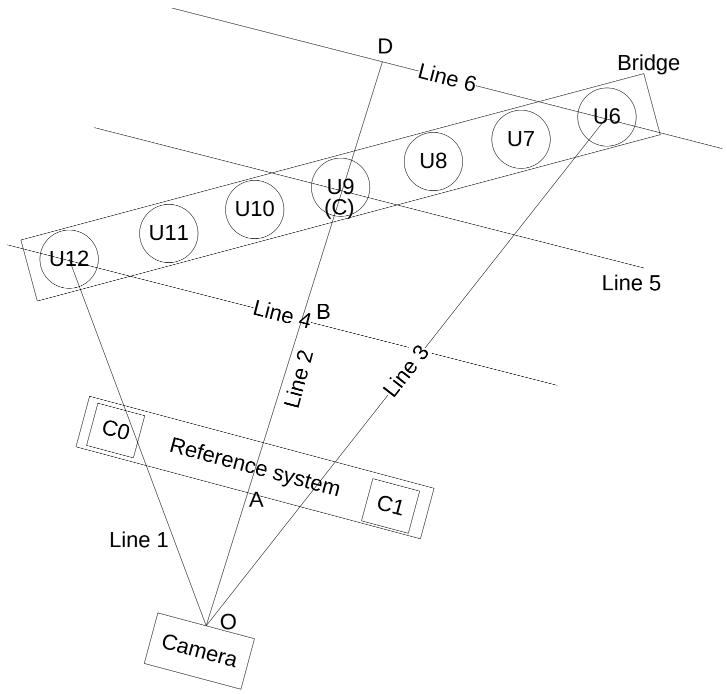

Fig. 5 - Illustration of the photographing scale transformation in the bridge test.

The photographing direction is perpendicular to the reference system, Line4, Line5, and Line6. Point A is the projection of Line 2 in reference system. Points B, C, and D are the intersections of Line 4 and Line 2, Line 5 and Line 2, Line 6 and Line 2, respectively. OB is the projection of Line1 in Line2 and OD is the projection of Line 3 in Line2.

Similarly, the approximate photographing scales of C0, C1, U7, U8, U10, and U11 were obtained. Table 3 shows the photographing scales of these reference points and deformation points on the bridge deck.

Tab. 3 - Photographing scales of C0-C1 and U6-U12/ (mm/pixel)

M_{C0}	M_{C1}	M_{U6}^{PST}	M_{U7}^{PST}	M_{U8}^{PST}	M_{U9}^{PST}	M_{U10}^{PST}	M_{U11}^{PST}	M_{U12}^{PST}
1.65	1.65	28.93	25.86	22.79	19.70	17.51	15.32	13.14

Measurement accuracy

In theory, reference points did not move during the test and their displacements were zero. However, the displacements of these reference points obtained by the PST-TBP method were not zero. These displacement values of these reference points can therefore be used to represent the measurement accuracy. Table 4 shows that the maximal error is 1.65mm in monitoring the reference points.

As image matching is the key to this monocular digital photography, we measured the image coordinates of these deformation points on the zero image times to assess its image matching accuracy. Table 5 shows that the maximal error was 1 pixel, and the minimal error was 0 pixels. The average errors of U6-U12 were 0.1 pixels, 0.1 pixels, 0 pixels, 0.3 pixels, 0 pixels, 0.3 pixels and 0.2 pixels, respectively. This method reached a sub-pixel Image matching accuracy.

Based on Table 3, it was obtained that the deflection errors of U6-U12 were 2.89 mm, 2.59 mm, 0 mm, 5.91 mm, 0 mm, 4.60 mm, 2.63 mm. The maximal and average deflection errors were 5.91 mm and 1.86 mm, respectively.

Tab. 4 - Measurement errors of reference points/mm

Point	Test1	Test2	Test3	Test4	Test5	Test6	Test7	Test8	Test9	Test10
C0	0.00	0.00	0.00	1.65	1.65	0.01	0.00	0.00	0.00	0.01
C1	0.01	0.00	0.00	0.00	0.00	1.64	0.00	0.00	0.00	0.00

Tab. 5 - Image matching errors of deformation points/pixel

Test	U6	U7	U8	U9	U10	U11	U12
1	1	0	0	0	0	1	0
2	0	0	0	1	0	0	1
3	0	0	0	1	0	0	0
4	0	0	0	1	0	1	0
5	0	0	0	0	0	1	0
6	0	0	0	0	0	0	1
7	0	0	0	0	0	0	0
8	0	0	0	0	0	0	0
9	0	1	0	0	0	0	0
10	0	0	0	0	0	0	0
Average	0.1	0.1	0	0.3	0	0.3	0.2

Analysis of bridge deflection trends

We calculated the pixel displacements (Table 6) and space displacements of some deformation points (Table 7). The positive and negative values (Tables 6 and 7) represent the deformation point moving up and down, respectively. The deformation points on the bridge deck (U6-U12) were chosen as the aim of this paper is to study the bridge deflection trends caused by vehicle dynamic load. Table 7 shows that in Test 6 deformation point U7 developed the maximal deflection-55.34 mm which was within the allowed value-75mm (the allowed value = the bridge span/800, where L = 60 m in this study).

Tab. 6 - Pixel displacements of U6-U12/pixel

Test	U6	U7	U8	U9	U10	U11	U12
1	-1.07	-0.76	-1.26	-0.44	-1.06	-1.53	-0.52
2	-1.18	-1.96	-1.65	-1.04	-0.88	-1.65	-1.21
3	-1.18	-0.95	-0.65	-1.03	-0.87	-0.65	-1.20
4	-0.18	-0.95	-0.65	-1.03	-0.88	-1.65	-1.19
5	-0.53	0.46	-0.46	-0.12	-0.35	-1.71	-1.24
6	-1.28	-2.14	-2.02	-1.60	-1.68	-1.76	-1.86
7	-1.17	-0.95	-1.64	-1.03	-0.87	-1.65	-0.20
8	-0.62	-0.72	-0.82	-0.68	-2.15	-1.81	-1.89
9	-0.18	0.04	-0.65	-1.03	-0.87	-0.65	-1.20
10	-1.17	-0.96	-0.64	-1.02	-0.87	-0.65	-1.19

Tab. 7 - Space displacements of U6-U12/mm

Test	U6	U7	U8	U9	U10	U11	U12
1	-30.96	-19.65	-28.72	-8.67	-18.56	-23.44	-6.83
2	-34.14	-50.69	-37.60	-20.49	-15.41	-25.28	-15.90
3	-34.14	-24.57	-14.81	-20.29	-15.23	-9.96	-15.77
4	-5.21	-24.57	-14.81	-20.29	-15.41	-25.28	-15.64
5	-15.33	11.90	-10.48	-2.36	-6.13	-26.20	-16.29
6	-37.03	-55.34	-46.04	-31.52	-29.42	-26.96	-24.44
7	-33.85	-24.57	-37.38	-20.29	-15.23	-25.28	-2.63
8	-17.94	-18.62	-18.69	-13.40	-37.65	-27.73	-24.83
9	-5.21	1.03	-14.81	-20.29	-15.23	-9.96	-15.77
10	-33.85	-24.83	-14.59	-20.09	-15.23	-9.96	-15.64

Deflection curves (Figures 6 and 7) were also depicted in order to visually analyse the bridge deflection law caused by vehicle dynamic load. Figure 6 shows that the deflection of every position on the bridge’s major structure was inelastic, all of which was within the bridge allowed value. Figure 7 shows that vehicle dynamic load results in the bridge moving down in spite of U7 moving up in test 5 and 7. In addition, the bridge global deflection curves fluctuated up and down like some sinusoidal-cosinusoidal curves. The bridge deflection was a parabola when the excavator moved to the bridge centre (Test 6). Especially, the deflection of every position on the bridge almost reached its maximal when the excavator moved to the bridge centre, which conforms to the deformation characteristics of the bridge caused by the external load.

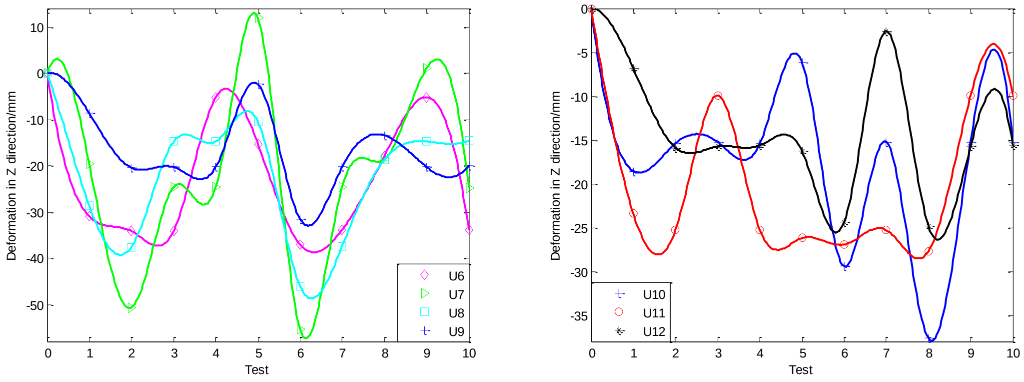

Fig. 6 - Deflection curves of deformation points on the bridge

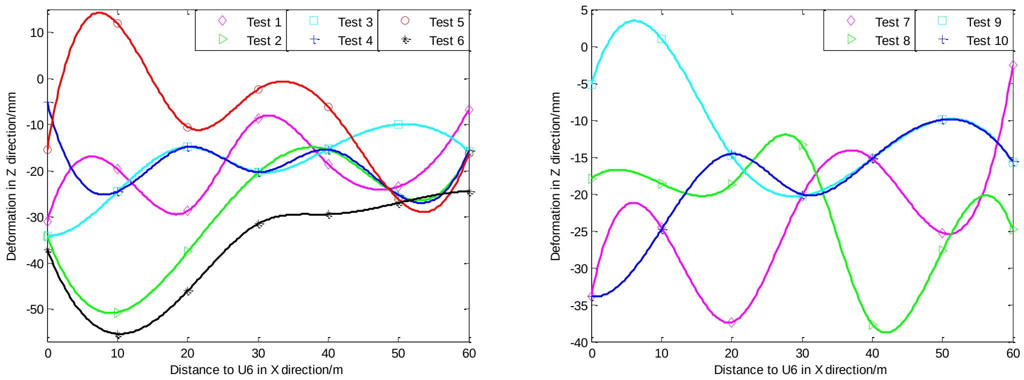

Fig. 7 - Global deflection curves of the bridge

Note that it is impossible to monitor the bridge deflection with high accuracy when the camera is far from the bridge. But it can provide data support to study the deflection deformation law of the bridge caused by vehicle dynamic load. Although we cannot get the precise deflection of the bridge, the deflection trend of the bridge is also an important indicator to assess the bridge health. In the future, MDP & MR (monocular digital photography and measurement robot) would be a useful method to monitor the global deflection of the bridge as the measurement robot can monitor precise short periodic deflection of the bridge, and MDP can monitor the global deflection trend of the bridge.

CONCLUSION

This study used MDP based on the PST-TBP method to monitor the dynamic global deflection of a bridge. Before the bridge test, we first set SONY350 cameras in proper place and levelled them. Then, the reference system, formed by reference points, perpendicular to the photographing direction, was set near the selected camera. We produced a zero image using the cameras to shoot the bridge before the test and produced image sequences by shooting the bridge every two seconds when the excavator was moving on the bridge. Through the results, the following conclusions are obtained:

(1) The PST-TBP method reaches a sub-pixel image matching accuracy. The average image matching error was within 0.3 pixels. And the maximal error was 1.65mm and 5.91 mm in monitoring the reference points and dynamic global deflection of a bridge, respectively.

(2) Every position of the bridge almost reaches the maximal deflection when the excavator moves to the bridge centre. The maximal deflection of the bridge was 55.34mm which was within the bridge allowed value-75mm.

(3) The deflection curves of the bridge fluctuated up and down like some sinusoidal-cosinusoidal curves. The bridge deflection was a parabola when the excavator moved to the bridge centre.

(4) Deflections of every position on the bridge were inelastic, all of which was within the bridge allowed. This indicates that the bridge is in good health.

The MDPS (monocular digital photography system) used in this study can monitor the dynamic global deflection of a bridge. Deflection trends of the bridge depicted by this system in real time show the bridge deflection visually, which is effective in warning the possible danger of the bridge. Although it cannot get the precise bridge deflection when the camera is far from the bridge, the dynamic deflection trend of the bridge is also an important indicator to assess the bridge health. In the future, MDP & MR (monocular digital photography and measurement robot) would be a useful method to monitor the bridge deflection as it can get precise short periodic deflection deformation of the bridge and the dynamic global deflection trend of the bridge.

ACKNOWLEDGEMENTS

This study was supported by the National Natural Science Foundation of China (Grant No.: 51674249), the Science and Technology project of Shandong province of China (Grant No.: 2010GZX20125).

REFERENCES

[1] X. M. Hou, X. S. Yang, Z. P. Liao, and S. L. Ma, "Bridge deflection real time measurement," *Earthquake Engineering & Engineering Vibration,* vol. 22, pp. 67-72, 2002.

[2] X. L. He and L. Z. Zhao, "Based on Inclinometer to Measure Dynamic Deflection of High-Speed Railway Bridge," *Applied Mechanics & Materials,* vol. 405-408, pp. 3019-3026, 2013.

[3] I. Lipták, A. Kopáčik, J. Erdélyi, and P. Kyrinovič, "Dynamic Deformation Monitoring of Bridge Structure," *Selected Scientific Papers - Journal of Civil Engineering,* vol. 8, pp. 13-20, 2013.

[4] D. H. Parker, B. Radcliff, and J. W. Shelton, "Advances in hydrostatic leveling with the NPH6, and suggestions for further enhancements," *Precision Engineering,* vol. 29, pp. 367-374, 2005.

[5] K. Y. Koo, J. M. W. Brownjohn, D. I. List, and R. Cole, "Structural health monitoring of the Tamar suspension bridge," *Structural Control & Health Monitoring,* vol. 20, pp. 609–625, 2013.

[6] P. A. Psimoulis and S. C. Stiros, "Measuring Deflections of a Short-Span Railway Bridge Using a Robotic Total Station," *Journal of Bridge Engineering,* vol. 18, pp. 182-185, 2013.

[7] Z. Xia, F. U. Hong qiao, W. Zhang, W. M. Chen, and Chongqing, "Modulation Transfer Function of Image Monitoring System for Bridge's Deformation," *Journal of Chongqing University,* 2004.

[8] H. Dong, W. M. Chen, F. U. Yu mei, and Chongqing, "Method of laser & imaging deflection measurement," *Journal of Transducer Technology,* 2004.

[9] X. Hou, X. Yang, and Q. Huang, "Using Inclinometers to Measure Bridge Deflection," *Bridge Construction,* vol. 10, pp. 564-569, 2004.

[10] V. Ashkenzai and G. W. Roberts, "EXPERIMENTAL MONITORING OF THE HUMBER BRIDGE USING GPS," in *Institution of Civil Engineers: Civil Engineering*, 1997, pp. 177-182.

[11] Y. Xie, "Inertial Measurement Method for Railway Bridge Dynamic Deflection," *Chinese Journal Ofentific Instrument,* 1999.

[12] J. F. Stanton, M. O. Eberhard, and P. J. Barr, "A weighted-stretched-wire system for monitoring deflections," *Engineering Structures,* vol. 25, pp. 347-357, 2003.

[13] Y. Liu, Y. Deng, and C. S. Cai, "Deflection monitoring and assessment for a suspension bridge using a connected pipe system: a case study in China," *Structural Control & Health Monitoring,* vol. 22, pp. 1408-1425, 2015.

[14] M. A. R. Cooper and S. Robson, "HIGH PRECISION PHOTOGRAMMETRIC MONITORING OF THE DEFORMATION OF A STEEL BRIDGE," *Photogrammetric Record,* vol. 13, pp. 505-510, 2006.

[15] C. Forno, S. Brown, R. A. Hunt, A. M. Kearney, and S. Oldfield, "Measurement of deformation of a bridge by Moire photography and photogrammetry," *Strain,* vol. 27, pp. 83-87, 2008.

[16] H. G. Maas, "Photogrammetric techniques for deformation measurements on reservoir walls," 1998.

[17] Y. H. Yu, C. Vo-Ky, S. Kodagoda, and Q. P. Ha, "FPGA-Based Relative Distance Estimation for Indoor Robot Control Using Monocular Digital Camera," vol. 14, pp. 714-721, 2010.

[18] V. Gorbatsevich, Y. Vizilter, V. Knyaz, and S. Zheltov, "Face Pose Recognition Based on Monocular Digital Imagery and Stereo-Based Estimation of its Precision," *International Archives of the Photogrammetry Remote Sensing & S,* vol. XL-5, pp. 257-263, 2014.

[19] R. R. P. D. Samuel, *close-range photogrammetry*: Springer Berlin Heidelberg, 2014.

[20] F. B. Bales, "CLOSE-RANGE PHOTOGRAMMETRY FOR BRIDGE MEASUREMENT," *Transportation Research Record,* vol. 1, 1984.

[21] K. Leitch, "CLOSE-RANGE PHOTOGRAMMETRIC MEASUREMENT OF BRIDGE DEFORMATIONS," *https://www.lap-publishing.com/,* 2010.

[22] F. Remondino, "Image Sequence Analysis For Human Body Reconstruction," *Archives of P & Rs,* vol. 34, pp. 590--595, 2002.

[23] N. D'Apuzzo, "Surface measurement and tracking of human body parts from multi-image video sequences," *ISPRS Journal of Photogrammetry and Remote Sensing,* vol. 56, pp. 360-375, 8// 2002.

[24] S. Yoneyama, A. Kitagawa, S. Iwata, K. Tani, and H. Kikuta, "BRIDGE DEFLECTION MEASUREMENT USING DIGITAL IMAGE CORRELATION," *Experimental Techniques,* vol. 31, pp. 34–40, 2007.

[25] P. Olaszek, "Investigation of the dynamic characteristic of bridge structures using a computer vision method," *Measurement,* vol. 25, pp. 227-236, 1999.

[26] A. Goktepe and E. Kocaman, "Using Direct Linear Transformation Method in X-Ray Photogrammetry and an Illustrative Study," *Experimental Techniques,* vol. 36, pp. 21–25, 2012.

[27] "Study of the Bridge Deformation Monitoring Technique and its Survey Specification," *Marine Environment & Engineering,* 2011.

[28] M. C. Lu, C. C. Hsu, and Y. Y. Lu, "Distance and angle measurement of distant objects on an oblique plane based on pixel variation of CCD image," in *Instrumentation and Measurement Technology Conference (I2MTC), 2010 IEEE*, 2010, pp. 318 - 322.

[29] C. C. J. Hsu, M. C. Lu, and Y. Y. Lu, "Distance and Angle Measurement of Objects on an Oblique Plane Based on Pixel Number Variation of CCD Images," *IEEE Transactions on Instrumentation & Measurement,* vol. 60, pp. 1779-1794, 2010.

[30] C. Mingzhi, Y. ChengXin, X. Na, Z. YongQian, and Y. WenShan, "Application study of digital analytical method on deformation monitor of high-rise goods shelf," in *2008 IEEE International Conference on Automation and Logistics*, 2008, pp. 2084-2088.